Seasonal variation of meteor decay times observed at King Sejong Station (62.22°S, 58.78°W), Antarctica

Jeong-Han Kim [a,b], Yong Ha Kim [a,*], Chang-Sup Lee [a], Geonhwa Jee [b]

[a] *Department of Astronomy and Space Science, Chungnam National University, 79 Daehangno, Yuseong-gu, Daejeon 305-764, Republic of Korea*
[b] *Korea Polar Research Institute, 7-50 Songdo-dong, Yeonsu-gu, Incheon 406-840, Republic of Korea*

ABSTRACT

We analyzed meteor decay times measured by a VHF radar at King Sejong Station by classifying strong and weak meteors according to their estimated electron line densities. The height profiles of monthly averaged decay times show a peak whose altitude varies with season at altitudes of $80-85$ km. The higher peak during summer is consistent with colder temperatures that cause faster chemical reactions of electron removal. By adopting temperature dependent empirical recombination rates from rocket experiments and meteor electron densities of $2 \times 10^5 - 2 \times 10^6$ cm^{-3} in a decay time model, we are able to account for decreasing decay times below the peak for all seasons without invoking meteor electron removal by hypothetical icy particles.

© 2010 Elsevier Ltd. All rights reserved.

1. Introduction

Meteors entering the earth's atmosphere reveal much information on the atmosphere through the process of interacting with increasingly dense air molecules, especially in the altitude region between 70 and 110 km, where most meteors ablate. Right after an ionized trail is produced as the meteor passes through the atmosphere, it begins to dissipate by several processes such as ambipolar diffusion, eddy diffusion, recombination, and chemical interaction with major neutral species in the background. Meteor radars detect echoes reflected from the trails as they decay with time, and evolution of the meteor echoes can be used to investigate characteristics of the mesosphere and lower thermosphere (MLT). The decay time of meteor echo has been used to estimate temperatures near the mesopause region in previous studies (Hocking et al., 1997; Hocking, 1999; Cervera and Reid, 2000; Singer et al., 2004; Hocking, 2004b; Stober et al., 2008).

The temperature estimation from meteor decay time assumes that ambipolar diffusion is the main trail expansion process in the early stage of meteor growth (McDaniel and Mason, 1973; Jones, 1975; Hocking et al., 1997), and that measured decay time is inversely proportional to ambipolar diffusion coefficient. The ambipolar diffusion coefficient has been known to be related to atmospheric temperature and pressure (Chilson et al., 1996; Hocking et al., 1997). Hocking (1999) proposed a method for

determining temperature near the mesopause region without pressure information, using the slope of logarithmic inverse decay time against altitude and temperature gradient. This method is valid only near the mesopause altitude, where the slope of decay time profile is well defined and temperature gradient is small. Temperatures inferred from meteor radar are reported to be reasonably consistent with those observed from other optical instruments on ground (Hocking et al., 2004a; Singer et al., 2004; Stober et al., 2008). Radar instruments have the advantages of being relatively immune to weather condition and it is possible to operate them during day and night continuously, unlike other ground-based optical instruments.

However, it is known that in the region above about 100 km, decay of meteor trails does not reflect the atmospheric condition coherently because the geomagnetic field distorts meteor trail diffusion very much in the low density region. Using a numerical method, Jones (1991) suggested that above the altitude of about 95 km the geomagnetic effect is important for decay of meteors, while Dyrud et al. (2001) mentioned this as about 100 km from plasma simulation. Hocking (2004c) proposed that modeling of meteor trail diffusion for altitudes above 93 km should consider the effect by geomagnetic field.

Below the altitude of about 95 km, meteor decay times increase with decreasing altitude, which can be accounted for by ambipolar diffusion of meteor trails since diffusion becomes slower (thus longer decay time for the meteor trail) at low altitudes due to denser atmosphere. However, recent meteor radar observations reported that meteor decay times decrease with decreasing altitudes below about 85 km, especially at high latitude stations (Hall et al., 2005; Singer et al., 2008; Younger

et al., 2008; Ballinger et al., 2008). The decreasing trend at low altitudes is opposite to the behavior of ambipolar diffusion. The observational studies analyzed height profiles of meteor decay time only above 80 km and simply suggested the idea that the decreasing trend below about 85 km may be due to the additional removal of meteor trail electron by icy and dust particles and ion–electron recombination process (Havnes and Sigernes, 2005; Singer et al., 2008; Younger et al., 2008; Ballinger et al., 2008). In this paper, we present seasonally varying height profiles of meteor decay times between 70 and 95 km observed at a southern high latitude station, and attempt to explain quantitatively the observed height profiles with a model that includes ambipolar diffusion and empirical electron recombination. We also discuss the possibility that icy particles are capturing meteor electrons, thus reducing decay times below about 85 km.

2. Observation and analysis

We have been operating a VHF meteor radar since its installation on March 2007 at King Sejong Station (62.22°S, 58.78°W). The VHF meteor radar supplied by ATRAD is an all-sky interferometric radar, which consists of 1 transmitting antenna, 5 receiving antennas, transmitter, and control and data acquisition system. A radio signal transmitted from the transmitting antenna is reflected by a meteor plasma trail, and the returning meteor echo signal is received by 5 receiving antennas simultaneously on ground with a range resolution of 2 km. Interferometric analysis of the received echo signal allows one to figure out the position of a meteor in the sky at an angular resolution of less than 2°. The radar operates with a maximum power of 8 kW at 33.2 MHz and detects meteor echoes continuously around the clock. The radar provides us with important pieces of information on a meteor itself and the atmosphere surrounding the meteor, such as Doppler drift speed of line of sight, the position of detected meteor in the sky, meteor decay time, and wind field. Details about ATRAD meteor radars have been described in Holdsworth et al. (2004, 2008), including 16 criteria for determining whether the signal is reflected by underdense meteor ionized trail or not.

The meteor radar has been detecting 15,000−28,000 meteors per day and the number of meteors varies with season. In this study, we analyzed data from March 2007 through July 2009, which make up a full year of data set after excluding maintenance breaks and months with small operating days. Table 1 lists numbers of operating days each month and numbers in boldface are number of days used in our analysis. The data set includes 26–31 days in a month except January, in which data were available only for 17 days. We selected unambiguous underdense meteor echoes with zenith angle between 10° and 70° to increase data reliability because data outside this range of zenith angle may contain significant uncertainties due to unspecular reflection, increase of error in height estimation with increasing zenith angles, and atmospheric effects near the horizon. We then divided the meteor data into two groups, strong and weak meteors
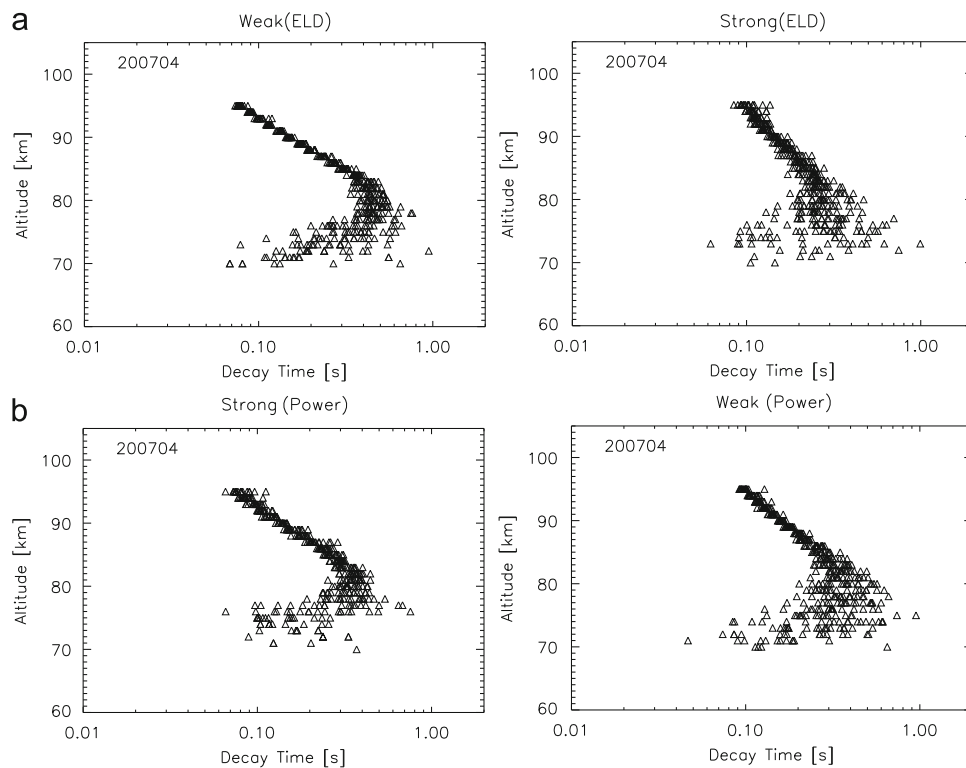
Table 1
Operating days of the meteor radar at King Sejong Station. Numbers in boldface are numbers of days used in the analysis.

	Jan.	Feb.	Mar.	Apr.	May	Jun.	Jul.	Aug.	Sep.	Oct.	Nov.	Dec.
2007			**29**	**30**	**31**	3	–	–	–	–	24	**29**
2008	9	–	–	–	6	5	12	**31**	**29**	**28**	**26**	17
2009	**17**	**28**	29	28	19	**30**	**28**	25				

Fig. 1. Height profiles of observed meteor decay times for April 2007. Each triangle represents a 15-min averaged value of observed decay times. (a) Strong and weak meteors are selected as the highest and lowest 25% q values in the monthly data set. The q value represents electron line density of a meteor trail (see text). (b) Strong and weak echoes are selected as the highest and lowest 25% of received powers in the monthly data set.

according to estimated relative electron line density, q, along the meteor trail as in Singer et al. (2008):

$$q \propto (\text{received power} \times \text{range}^3)^{0.5} \qquad (1)$$

where received power is the strength of signal reflected from meteor trail in dB unit and range the distance between the receiving antenna and meteors reflecting the signal. The original form of this equation was suggested in McKinley (1961) and included parameters such as transmitted power, antenna directivity, and radar wavelength (λ). However, our purpose of classifying echoes requires only a relative electron line density deduced from the above relation. According to this equation, the strong meteor was defined here by the highest 25% of q value in the monthly data set, while the weak meteor was by the lowest 25%. We then took average of meteor decay times from each group for a 15-min period at the same local time between 11:00LT and 16:00LT during a month, assuming that the background atmosphere is in the same condition at the same local time during a month. Numbers of meteors used for the 15 min average are up to about 200, depending on altitude. Fig. 1 shows the 15 min averaged decay times, which represent monthly height profiles of decay times. The meteor decay time is here defined as the time, $\tau_{1/2}$, over which amplitude of reflected signal falls to one half of its maximum amplitude. We have also plotted decay times for nighttime in the same way (not shown), but they are of no significant difference from those for daytime.

Younger et al. (2008) classified strong and weak echoes according to the received power only. In this case, strong (weak) echoes generally fall into our definition of weak (strong) meteor since our definition of the group is dependent mainly on range rather than received power. A comparison of these two definitions is shown in Fig. 1, where the upper panels are by the electron line density criterion and the lower panels are by the received power criterion. Echoes with long range usually have small received powers due to attenuation along the round trip of radar signal to the meteors, but they represent strong electron line densities of the meteor trail if they still have detectable signal power despite the attenuation along the round trip. We use the line density criterion to characterize strong and weak meteors because electron line density of the trail is critical to understand meteor decay time process.

3. Results and discussion

3.1. Height profiles of observed meteor decay times

Fig. 2 shows height profiles of the observed meteor decay times for January and July 2009, April 2007, and October 2008, representing southern summer, winter, fall, and spring, respectively. Each plus symbol indicates a 15-min averaged value with the 1 km altitude bin, and monthly mean decay times at each altitude bin are marked with triangles. For weak meteors (left panels), the height profiles form a very narrow line that increases with decreasing altitudes down to 80–85 km depending on season. For strong meteors (right panels), decay times also increase with decreasing altitude down to about 85 km, but they are much more scattered than for weak meteors. Increasing decay times with decreasing altitude can be accounted for by ambipolar diffusion of ionized meteor trail since diffusion becomes slower due to increasing atmospheric densities with decreasing altitude. Using the weak meteors only, we can estimate atmospheric temperatures in this altitude region from diffusion coefficients that fit the slope of observed decay times, better than in Hocking (1999) since they included strong meteors, making it difficult to define the slope of decay times.

Decay times below about 85 km are broadly scattered, but monthly mean decay times clearly decrease with decreasing altitude, especially for weak meteors. The decreasing trend in this altitude region is opposite to the behavior of ambipolar diffusion. Turning altitude of the height profiles seems to vary with season—at about 85 km during southern summer and about 80 km during other seasons. The decreasing trend of decay time was first reported by Hall et al. (2005), and has been noted by a few recent studies (Singer et al., 2008; Younger et al., 2008; Ballinger et al., 2008). Singer et al. (2008) analyzed meteor decay times in the altitude range of 81–95 km and reported a decreasing trend below about 85 km during summer season at both northern and southern high latitude regions. They speculated that decreasing decay time may be related with the occurrence of icy particles, which may result from the noctilucent cloud (NLC) near coldest summer mesopause region. In our observations, however, the decreasing trend of meteor decay times below about 85 km seems persistent during all seasons although the turning altitude varies with season.

While previous studies analyzed meteor decay times above about 80 km (Hocking et al., 1997; Hocking, 1999; Hocking and Hocking, 2002; Singer et al., 2004, 2008; Younger et al., 2008), we included the data in the $70-80$ km altitude region in our analysis in order to further investigate the behavior of decay times below 80 km altitude. There are about 4% of meteors detected in the $70-80$ km region over King Sejong Station. Data in the $70-80$ km region are critical to understand the decreasing trend of meteor decay time in terms of various electron removal processes other than ambipolar diffusion, as will be discussed in the following sections.

3.2. Modeling of meteor decay time

Although it has been mentioned in several studies that the decreasing trend of decay times at low altitudes may be caused by additional removal processes of electrons in meteor trail by icy and dust particles associated with NLC, or/and recombination of electrons in trail (Singer et al., 2008; Younger et al., 2008; Ballinger et al., 2008), any quantitative model has not been suggested. One of the important characteristics of the mesosphere is that both positive and negative ions exist, and it is possible to produce water cluster ions by active three-body reaction process due to relatively high atmospheric density (Wisemberg and Kockarts, 1980; Kull et al., 1997; Schunk and Nagy, 2000; Raizada et al., 2008). Hence not only icy particles suggested by previous studies but also D-region chemistry governing this region may significantly affect meteor decay times at low altitudes.

In order to explain the behavior of decay time with height between 70 and 95 km obtained from our meteor radar observation, we propose that removal of meteor trail electrons by mesospheric ion chemistry plays an important role in the meteor trail decay process, in addition to ambipolar diffusion. The removal of meteor electron by ion chemistry can be addressed by empirical recombination coefficients measured by rocket experiments, as summarized in Friedrich et al. (2004). We adopt the empirical recombination rates, α_{eff}, for daytime condition with temperature dependencies at 5 mesospheric altitudes, which are presented in Friedrich et al. (2004). The adopted empirical recombination rates are $1.3-1.6 \times 10^{-7}$ cm^3 s^{-1} for $T = 180-140$ K at 93 km and increase up to $1.3-2.0 \times 10^{-5}$ cm^3 s^{-1} for $T = 250-230$ K at 65 km. For a given temperature and altitude, interpolated values were computed from 5 sets of the temperature dependent recombination rates between 65 and 93 km. The empirical recombination rates represent loss rates of electrons via recombination reactions not only with molecular
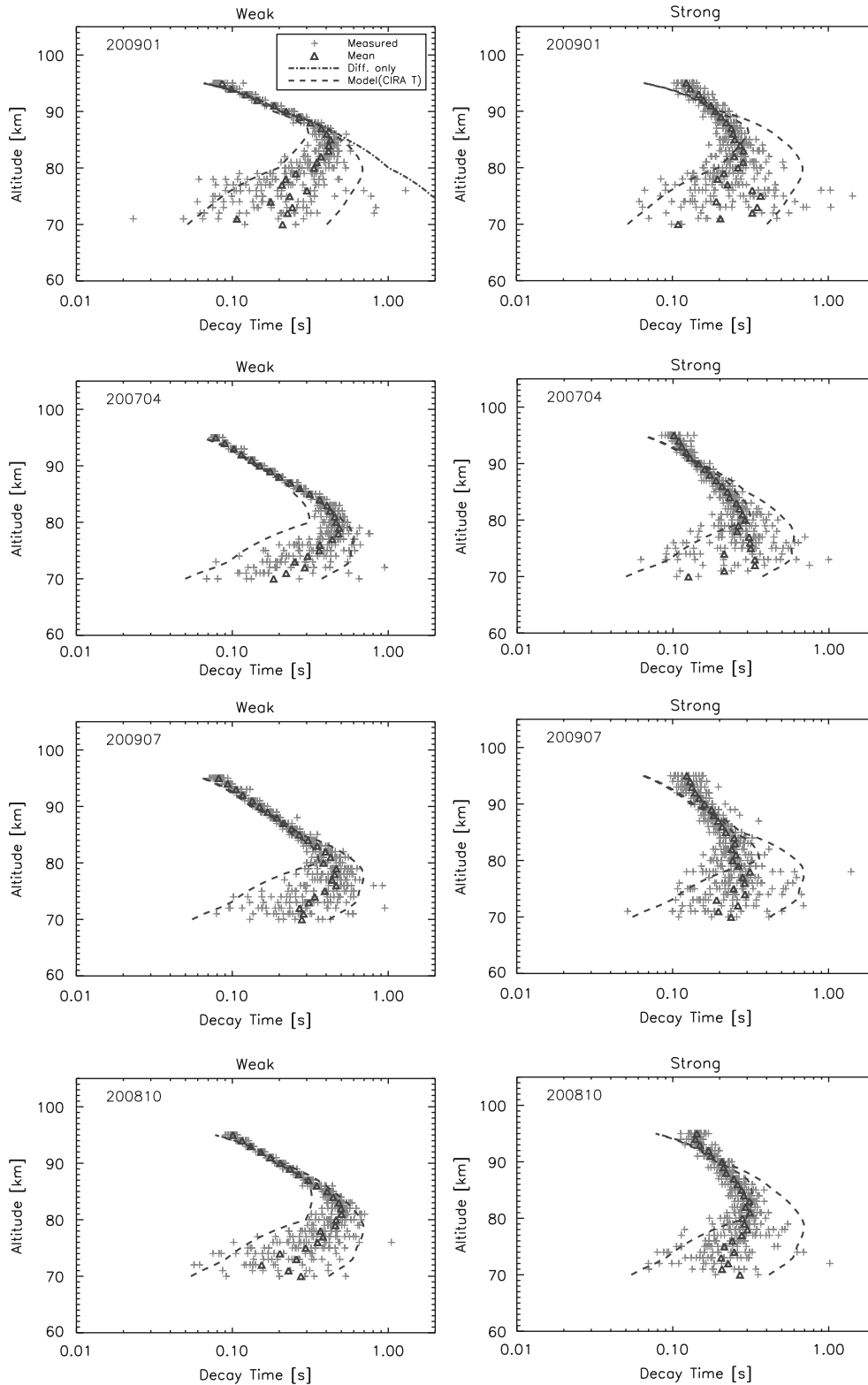
Fig. 2. Height profiles of observed meteor decay times (light plus signs and dark triangles). Model decay times are overlapped with dashed lines for January, April, July, and October. The long and short model decay time profiles are for electron densities of 2.5×10^5 and $2.2 \times 10^6 \, cm^{-3}$ in the meteor trails, respectively. A diffusion only model is also presented with a dash–dotted line for the January weak meteor case.

ions but also with cluster ions, whose rates are orders of magnitude larger. Formation of cluster ions is strongly dependent on atmospheric densities, which makes empirical recombination rates to increase with decreasing altitudes. Furthermore, three-body electron attachment could contribute to empirical

recombination rates. It is necessary to note that empirical recombination rates are primarily based on rocket flight measurements, which were mainly performed at northern high latitude regions (Torkar and Friedrich, 1988; Friedrich et al., 2004). All chemical rates (recombination with molecular ions and

cluster ions, electron attachment, clustering) have negative temperature dependencies (lower temperature higher empirical recombination rate).

We propose that meteor decay time can then be expressed with a combination of ambipolar diffusion and empirical electron recombination as

$$\tau_{1/2} = \frac{1}{f(D_a/\lambda^2) + n_e \alpha_{eff}} \qquad (2)$$

Here D_a and f are the ambipolar diffusion coefficient and a correction factor for computed D_a, respectively, λ is the radar wavelength, and n_e is an estimated electron density in a meteor trail. The ambipolar diffusion coefficient is known to be related to atmospheric temperature, T, and pressure, P (Chilson et al., 1996; Hocking et al., 1997):

$$D_a = \frac{16\pi^2}{\ln 2} \frac{2kT}{q_e} \left(\frac{T}{273.16}\right) \left(\frac{1.013 \times 10^5}{P}\right) K_0 \qquad (3)$$

where k is the Boltzmann constant, q_e the electronic charge, and K_0 the ion mobility in meteor trails. We adopted an ion mobility of $2.5 \times 10^{-4}\ \mathrm{m^2\ s^{-1}\ V^{-1}}$, assuming that metallic ion is dominant in meteor trail. A detailed discussion about ion mobility can be found in Jones and Jones (1990) and Chilson et al. (1996). D_a was computed with monthly mean temperatures and pressures of the CIRA86 empirical model (Fleming et al., 1988), which has a latitudinal resolution of $10°$ and vertical resolution of 5 km. We extracted the temperature and pressure applicable to the location of King Sejong Station from interpolated CIRA86 model values. It should be noted that CIRA86 model temperatures were lower than mesospheric temperatures measured by in-situ rocket-borne and falling sphere experiments performed at northern and southern high latitudes by up to about 20 K around the summer mesopause region, while the difference was less than about 10 K in the 70–80 km altitude region (Lübken and von Zahn, 1991; Lübken et al., 1999).

Although there have been several studies about electron line density in meteor trail, information on electron number density is very rare so far (Lovell, 1947; Lovell and Clegg, 1948). As nominal values, we deduced electron number densities from the minimum and maximum electron line densities for weak and strong meteors estimated by Singer et al. (2008), assuming a meteor radius of 1 m as used in other studies (Elford, 2001; Havnes and Sigernes, 2005). The deduced electron densities for weak and strong meteors are in the range 2.5×10^5–6.4×10^5 and 5.4×10^5–$2.2 \times 10^6\ \mathrm{cm^{-3}}$, respectively. Electron line densities in Singer et al. (2008) are slightly smaller than those in Lovell (1947), which were based on radar observations of the Perseid meteor shower.

3.3. Comparison between the observed and model decay times

Fig. 2 shows height profiles of three model decay times: two dashed and dash–dotted curves are for electron densities, n_e, of upper (left dashed curve), lower (right dashed curve), and zero values, respectively, in Eq. (2). We adopt the lower and upper values of 2.5×10^5 and $2.2 \times 10^6\ \mathrm{cm^{-3}}$, respectively, as mentioned in the previous section. The model profile with zero value ($n_e = 0$) is the diffusion only model, in which decay times increase with decreasing altitudes because ambipolar diffusion coefficient is inversely proportional to atmospheric pressure. The other model profiles deviate from the diffusion only model and have turning over around 80 km, depending on the value of n_e used in Eq. (2); higher n_e results in early turning over as altitude decreases.

For weak meteors in the range ~ 85–95 km, it is clear that model profiles are practically the same as those of the diffusion

only model and give good agreement with observed decay times. The weak meteors in this altitude region decay efficiently by ambipolar diffusion, which is consistent with the results of previous studies (e.g. Jones, 1975; Jones and Jones, 1990). In the case of strong meteors, however, observed decay times are longer than in the models above ~ 90 km and their slopes are steeper than those in the model above the turning altitude of the model profiles. This may indicate that diffusion process may not be efficient even at high altitudes probably due to relatively large plasma densities in strong meteor trails. In addition, large electron densities in the core of the trail may contribute to reducing decay times below ~ 90 km via effective recombination (cluster ions and attachment), resulting in steeper slopes in the decay time profiles than in the diffusion only model. The peaks of decay time profiles are shorter in strong meteors than in weak meteors for all months, implying fast decay by chemical reactions due to relatively large electron density in strong meteors. Note that decay times of strong meteors here are measured mostly from very weak signal due to long range detection, and thus may include an inherent bias for the measured values. In fact, decay times for strong meteors are distributed in relatively small range of times and their distribution is only marginally changed over season. Thus we limit our analysis to weak meteors in the following discussions.

In the left panels of Fig. 2, slopes of observed decay times in the region of ~ 80–95 km clearly show seasonal variation—slope is steeper during southern winter (July) than in summer in profiles of both weak and strong meteors, which is in good agreement with the result of Hocking (1999). Observed decay times form a very clear slope, which can be quantitatively compared with model profiles that were computed with CIRA temperatures and pressures. In other words, we can estimate temperature around 90 km from the slope of decay times for the weak meteors, as done in Hocking (1999).

A direct comparison between observed and model decay times at 90 km for weak meteors seems to suggest that CIRA temperature and pressures deviate from the actual ones over King Sejong Station. In order to match observed decay times at 90 km, our model requires a correction factor, f, in the range 0.54–1.04, the smallest and largest values being for winter (July) and summer (January), respectively. It is remarkable that the correction factor is close to unity despite the fact that the absolute value of diffusion coefficient is dependent on a rather uncertain physical parameter like ion mobility. The mean value for correction factors is 0.79, indicating that the assumed metallic ion mobility, $2.5 \times 10^{-4}\ \mathrm{m^2\ s^{-1}\ V^{-1}}$, is larger than the actual value. This is consistent with the fact that the meteor plasma trail is not purely metallic. If the CIRA pressures are exact at 90 km, a variation of correction factors of ± 0.25 from the mean may imply about $\pm 12\%$ deviation from the CIRA temperature since diffusion coefficient has T^2/P dependency. Using meteor radar, CIRA86 model, and lidar and satellite data, Hocking et al. (1997) studied the seasonal variation of $T/P^{1/2}$ parameter, and also questioned about the accuracy of CIRA86 model temperatures and pressures, which have the vertical and latitudinal resolutions of 5 km and $10°$, respectively. We estimated temperatures at 90 km from the slope of decay times without assuming pressure—the estimated temperature is lower by as much as 50 K than the CIRA values during summer, which will be presented in a separate work with a comparison of temperatures inferred from OH and O_2 airglow measurements.

Fig. 2 shows that monthly mean decay times (indicated with triangles) have a peak at 80–85 km and decrease with decreasing altitude below the peak. Note that the model profile with diffusion only does not have the decay time peak since diffusion coefficient in Eq. (3) keeps decreasing with decreasing altitude.

The decreasing trend of monthly mean decay times is explained by the increasing trend of empirical recombination rates with decreasing altitude. Furthermore, monthly mean decay times seem to show a peak at higher altitude during southern summer than winter. This feature is consistent with the tendency that lower mesospheric temperatures during summer cause faster removal reactions of electrons due to negative temperature dependencies of chemical removal processes, such as recombination, attachment, and clustering, as reported by Friedrich et al. (2004). The model profiles explain this feature appropriately since seasonal temperature variation is reflected in empirical recombination rates, α_{eff}, i.e. larger values for cold summer than for warm winter.

It is remarkable that the two model profiles cover most of the observed decay times of weak meteors around and below the peak. However, the upper value for electron density, 2.2×10^6 cm^{-3}, in the model is about 3 times larger than that estimated from electron line density in Singer et al. (2008) for weak meteors. If we use the upper value, 6.4×10^5 cm^{-3}, from the estimation of Singer et al. (2008) for weak meteors, the model profiles would not cover about half of the observed decay times between 70 and 85 km, missing the shorter part of decay times. Alternatively, a three fold increase in empirical recombination rate, α_{eff}, would account for the discrepancy, but it may then require negative temperature perturbation of $60 - 40$ K from the assumed CIRA temperatures at $70 - 80$ km. The negative temperature perturbation seems to be unreasonably large for the $70 - 80$ km region, although gravity waves can perturb mesospheric temperatures of ~ 20 K in either direction from the mean temperature (e.g. Lübken and von Zahn, 1991). A temperature perturbation of 20 K by gravity waves can cause 50% and 70% variation in empirical recombination rate, α_{eff}, at 72.5 and 80 km, respectively, and may thus result in as much scatter of decay times from the mean values. The left panels of Fig. 2 show that the scatter of decay times around 70 km is up to about 300% from the mean value in either direction in January, and somewhat smaller in other seasons. Therefore, we argue that the scatter of measured decay times at 70–85 km is mostly due to variation in meteor trail electron densities, a wider variation than the range estimated from the minimum and maximum electron line densities of Singer et al. (2008) for weak meteors.

Previous studies speculated that the cold mesospheric temperature during polar summer may cause icy particles (may or may not be associated with the NLC), and these icy particles can capture electrons in the meteor trail. It was suggested that decreasing meteor decay times below the peak altitude may be due to electron capture of the icy particles. However, our analysis of meteor decay times at $70 - 85$ km does not need to invoke the icy particles to explain the decreasing trend even in the cold summer, although sub-visible icy particles may have minor contribution to the decay of meteor trails in the altitude region where temperature is low enough to form icy particles, especially during summer. If the icy particles exist to remove meteor trail electrons, the rate should be comparable to the inverse of measured decay times, ~ 1 s^{-1} in the $70 - 80$ km altitude region. Assuming a cross section of the icy particle, 10^{-12} cm^2 (10 nm diameter) and an electron thermal velocity, 10^7 cm s^{-1}, we may expect that number density of icy particles is about 10^5 cm^{-3} to account for the 1 s^{-1} removal rate. Reid (1997) suggested that 10 nm size dust particles with a density of 3×10^3 cm^{-3} can cause a bite-out in the electron density profile, where the polar mesospheric summer echo (PMSE) occurs. However, the PMSE altitudes are in the range $80 - 85$ km, higher than the altitudes where the additional decay process is needed in our analysis. Furthermore, icy particles may not survive below 80 km due to sublimation at warm temperatures. Since lidars have detected signals from NLC particles associated with PMSE, the 10 nm particles with a density of 10^5 cm^{-3} would have been detected with lidars and other optical instruments.

We note that sub-visible dust particles from meteors can act as scavengers for free electrons in the meteor trails at all seasons and in the whole mesosphere. However, it is hard to speculate that the characteristics and densities of meteor dusts vary with season just to match with our meteor decay time profiles. Effects of meteor dusts may be more important in the upper mesosphere region, where most meteors are ablaze.

4. Summary and conclusions

Observation of meteor echoes by a VHF meteor radar has been carried out at King Sejong Station, Antarctica, during the period March 2007 – July 2009. Height profiles of the observed meteor decay times between 70 and 95 km are analyzed through classification into strong and weak meteors according to their estimated electron line densities. The height profiles of monthly averaged decay times show a peak, whose altitude varies with season in the range $80 - 85$ km—higher peak in southern spring and summer than in fall and winter. The higher peak during summer is consistent with colder temperatures that cause faster chemical reactions of electron removal, such as molecular ion–electron recombination, cluster ion–electron recombination, and electron attachment.

The height profiles of 15-min averaged decay times show a clear increasing trend with decreasing altitude from 95 km to the peak altitudes, especially for weak meteors. This feature for weak meteors is well explained by ambipolar diffusion of meteor trails, which could allow estimation of atmospheric temperatures and pressures, as suggested by previous studies. However, the strong meteors show not only significant scatter but also different slope of the increasing trend from 95 km to the peak altitude. Therefore atmospheric temperature estimation from meteor decay times should be applied for weak meteors only.

Below the peak altitudes the observed decay times show a clear decreasing tendency with decreasing altitude, although there are large scatters from the averaged values at each altitude. The decreasing tendency cannot be explained by ambipolar diffusion, which becomes slower with decreasing altitudes due to increasing atmospheric densities. By adopting the empirical recombination of Friedrich et al. (2004) in a decay time model, we were able to account for the decreasing trend of meteor decay times for all seasons. Our model suggests that electron densities in weak meteor trails are in the range 2×10^5–2×10^6 cm^{-3}, of which the upper value is about 3 times larger than the estimation of Singer et al. (2008) for weak meteors. Shorter decay times measured during summer than other seasons can be explained by cold temperatures, which increase empirical recombination, without invoking hypothetical icy particles that were suggested by previous studies. The required number densities of icy particles would be inconsistent with non-detection of mesospheric cloud around $70 - 80$ km during Antarctic summer.

References

Ballinger, A.P., Chilson, P.B., Palmer, R.D., Mitchell, N.J., 2008. On the validity of the ambipolar diffusion assumption in the polar mesopause region. Annales Geophysicae 26 (11), 3439–3443.

Cervera, M.A., Reid, I.M., 2000. Comparison of atmospheric parameters derived from meteor observations with CIRA. Radio Science 35 (3), 833–843.

Chilson, P.B., Czechowsky, P., Schmidt, G., 1996. A comparison of ambipolar diffusion coefficients in meteor trains using VHF radar and UV lidar. Geophysical Research Letters 23 (20), 2745–2748.

Dyrud, L.P., Oppenheim, M.M., vom Endt, A.F., 2001. The anomalous diffusion of meteor trails. Geophysical Research Letters 28 (14), 2775–2778.

Elford, W.G., 2001. Novel applications of MST radars in meteor studies. Journal of Atmospheric and Solar–Terrestrial Physics 63 (2−3), 143–153.

Fleming, E.L., Chandra, S., Shoeberl, M.R., Barnett, J.J., 1988. Monthly mean global climatology of temperature, wind, geopotential height and pressure for 0–120 km. NASA Technical Memorandum, 100697.

Friedrich, M., Torkar, K.M., Steiner, R.J., 2004. Empirical recombination rates in the lower ionosphere. Advances in Space Research 34 (9), 1937–1942.

Hall, C.M., Aso, T., Tsutsumi, M., Nozawa, S., Manson, A.H., Meek, C.E., 2005. Testing the hypothesis of the influence of neutral turbulence on the deduction of ambipolar diffusivities from meteor trail expansion. Annales Geophysicae 23 (3), 1071–1073.

Havnes, O., Sigernes, F., 2005. On the influence of background dust on radar scattering from meteor trails. Journal of Atmospheric and Solar–Terrestrial Physics 67 (6), 659–664.

Hocking, W.K., Thayaparan, T., Jones, J., 1997. Meteor decay times and their use in determining a diagnostic mesospheric temperature–pressure parameter: methodology and one year of data. Geophysical Research Letters 24 (23), 2977–2980.

Hocking, W.K., 1999. Temperatures using radar-meteor decay times. Geophysical Research Letters 26 (21), 3297–3300.

Hocking, W.K., Hocking, A., 2002. Temperature tides determined with meteor radar. Annales Gephysicae 20 (9), 1447–1467.

Hocking, W.K., Singer, W., Bremer, J., Mitchell, N.J., Batista, P., Clemesha, B., Donner, M., 2004a. Meteor radar temperatures at multiple sites derived with SKiYMET radars and compared to OH, rocket and lidar measurements. Journal of Atmospheric and Solar–Terrestrial Physics 66 (6−9), 585–593.

Hocking, W.K., 2004b. Radar meteor decay rate variability and atmospheric consequences. Annales Geophysicae 22 (11), 3805–3814.

Hocking, W.K., 2004c. Experimental radar studies of anisotropic diffusion of high altitude meteor trails. Earth Moon and Planets 95 (1−4), 671–679.

Holdsworth, D.A., Reid, I.M., Cervera, M.A., 2004. Buckland Park all-sky interferometric meteor radar. Radio Science 39 (5), RS5009.

Holdsworth, D.A., Murphy, D.J., Reid, I.M., Morris, R.J., 2008. Antarctic meteor observations using the Davis MST and meteor radars. Advances in Space Research 42 (1), 143–154.

Jones, J., 1975. On the decay of underdense radio meteor echoes. Monthly Notices of the Royal Astronomical Society 173, 637–647.

Jones, W., Jones, J., 1990. Ionic diffusion in meteor trains. Journal of Atmospheric and Terrestrial Physics 52 (3), 185–191.

Jones, W., 1991. Theory of diffusion of meteor trains in the geomagnetic field. Planetary Space Science 39 (9), 1283–1288.

Kull, A., Kopp, E., Granier, C., Brasseur, G., 1997. Ions and electrons of the lower-latitude D region. Journal of Geophysical Research 102 (A5), 9705–9716.

Lovell, A.C.B., 1947. Electron density in meteor trails. Nature 160, 670–671.

Lovell, A.C.B., Clegg, J.A., 1948. Characteristics of radio echoes from meteor trails: I. The intensity of the radio reflections and electron density in the trails. Proceedings of the Physical Society 60, 491–498.

Lübken, F.-J., von Zahn, U., 1991. Thermal structure of the mesopause region at polar latitudes. Journal of Geophysical Research 96 (D11), 20841–20857.

Lübken, F.-J., Jarvis, M.J., Jones, G.O.L., 1999. First in situ temperature measurements at the Antarctic summer mesopause. Geophysical Research Letters 26 (24), 3581–3584.

McDaniel, E.W., Mason, E.A., 1973. The Mobility and Diffusion of Ions in Gases. John Wiley and Sons, New YorK.

McKinley, D.W.R., 1961. Meteor Science and Engineering. McGraw-Hill, New York.

Raizada, S., Sulzer, M.P., Tepley, C.A., Gonzalez, S.A., Nicolls, M.J., 2008. Inferring D region parameters using improved incoherent scatter radar techniques at Arecibo. Journal of Geophysical Research 113 (A12), A12302.

Reid, G.C., 1997. The nucleation and growth of ice particles in the upper mesosphere. Advances in Space Research 20 (6), 1285–1291.

Schunk, R.W., Nagy, A.F., 2000. Ionospheres: Physics, Plasma Physics, and Chemistry. Cambridge University Press, Cambridge.

Singer, W., Bremer, J., Weiβ, J., Hocking, W.K., Höffner, J., Donner, M., Espy, P., 2004. Meteor radar observations at middle and Arctic latitudes. Part 1: mean temperatures. Journal of Atmospheric and Solar–Terrestrial Physics 66 (6−9), 607–616.

Singer, W., Latteck, R., Millan, L.F., Mitchell, N.J., Fiedler, J., 2008. Radar backscatter from underdense meteors and diffusion rates. Earth, Moon and Planets 102 (1−4), 403–409.

Stober, G., Jacobi, Ch., Fröhlich, K., Oberheide, J., 2008. Meteor radar temperatures over Collm (51.3°N, 13°E). Advances in Space Research 42 (7), 1253–1258.

Torkar, K.M., Friedrich, M., 1988. Empirical electron recombination coefficients in the D- and E-region. Journal of Atmospheric and Terrestrial Physics 50 (8), 749–761.

Wisemberg, J., Kockarts, G., 1980. Negative ion chemistry in the terrestrial D region and signal flow graph theory. Journal of Geophysical Research 85 (A9), 4642–4652.

Younger, J.P., Reid, I.M., Vincent, R.A., Holdsworth, D.A., 2008. Modeling and observing the effect of aerosols on meteor radar measurements of the atmosphere. Geophysical Research Letters 35 (15), L15812.